CHEMICAL ENGINEERING TRANSACTIONS, Volume 11, 2007
Edited by Sauro Pierucci
 ISBN 978-88-95608-00-6

Role of a-periodic large scale flow structures in particle resuspension in stirred tanks

Valentina Lavezzo[a] , Marina Campolo[b] , Alfredo Soldati[a,b *]
[a] Dipartimento di Energetica e Macchine, and
[b] Centro Interdipartimentale di Fluidodinamica e Idraulica,
Università degli Studi di Udine 33100, Udine, Italy

The flow field generated by a rotating impeller is characterized by velocity variations with different spatial and temporal scales: (i) *large scales*, associated with impeller rotation and non-periodic fluctuations with episodic, bursting events often identified as macro-instabilities; (ii) *small scales* associated with turbulence. Flow motions associated with these different scales contribute to energy transfer, dissipation and also to mixing of species and to dispersion of suspended particles.

In this work we propose a methodology based on the concept of coherent flow structures to characterize the flow field in a stirred vessel. Our final aim is to identify the role of large scale flow structures in particle dispersion/resuspension dynamics.

To these aims we performed a Direct Numerical Simulation to obtain the turbulent flow field generated by an eight-blade paddle impeller placed mid-way between the top and the bottom of the tank, rotating at 100 rpm. A Lagrangian tracking approach has been used to reproduce the behavior of three swarms of 40 000 solid spherical particles of different diameter (30 μm, 50 μm and 100 μm) dispersed in the domain. (for further details see Sbrizzai et al., 2006).

Particles which are uniformly distributed in the flow at starting time tend to accumulate at the bottom of the tank in the close vicinity of the shaft where several strongly energetic bursting events, occurring in the simulated time period, produce significant particle resuspension. These events have been correlated to the Ekman pumping produced by a precessing vortex type instability. In this work we characterize the macro-instability associated with the Ekman pumping and we quantify its contribution to the resuspension of inertial particles.

1. Introduction

Many industrial applications use stirred-tanks to mix fluids or to suspend and disperse solid particles or gases.

Dispersion of species in a stirred tank is controlled by flow structures characterized by different length and time scales: (i) *large scales*, associated with impeller rotation and non-periodic fluctuations with episodic, bursting events often identified as macro-instabilities; (ii) *small scales* associated with turbulence. Flow motions associated with these different scales contribute to energy transfer and dissipation and are not equally effective in the dispersion of suspended particles. Additional insight in the mixing process is necessary to devise strategies for mixing optimization.

Many investigations based on both experiments and numerical simulations have been performed to identify the mechanisms promoting the generation of the large-scale structures and to capture the particle interaction/transport by large and small scales.
Ducci and Yianneskis, (2006) employed a vortex tracking methodology to accurately investigate by means of PIV and LDA techniques, the precession of macro-instability (MI) vortices in stirred vessels with different configurations. They demonstrated that the the knowledge of the MI vortex path may reduce considerably the mixing time. Galletti et al., (2005) focused their analysis on the different types of instabilities that are present in most stirred tanks: precessional (MI) and impeller stream flow instabilities. They calculated the energy of such instabilities through two-point LDA measurements, and showed that understand their magnitude and frequency would provide methodologies for the design of more efficient operations. Nikiforaki et al., (2003) studied different vessel configurations by means of LDA and found that MI frequencies, related to the rotational speed velocity N, are in the range of 0.015-0.02N (Hz).
Numerical simulations have been employed mainly to test experimental results as in Hartmann et al., (2004) and Roussinova et al., (2003) who performed Large Eddy Simulation (LES) to calculate frequency and nature of the macro-instabilities.
A Direct Numerical Simulation is employed in this work to obtain the turbulent flow field generated by an eight-blade paddle impeller (C/H=0.5) and to understand the role of a precessional vortex type instability (Ekman pumping effect) in particle mixing dynamics. Lagrangian tracking of different diameter particles (30 μm, 50 μm and 100 μm) has shown that particles uniformly distributed in the flow at starting time tend to accumulate at the bottom of the tank in the close vicinity of the shaft where strongly energetic bursting events re-suspend them (for further details see Sbrizzai et al., 2006).
Objectives of our research are: (i) to identify the large-scale flow structures responsible for particle re-suspension, (ii) to propose a new methodology based on the concept of coherent flow structures to characterize the macro-instability associated with the Ekman pumping and (iii) to quantify its contribution to the re-suspension of inertial particles.

2. Methodology

2.1 Flow field

Navier-Stokes equations are solved in a cylindrical reference frame for the reactor geometry shown in Figure 1. Dimensions of vessel/impeller are made dimensionless using the impeller radius L_r =1.25 cm, L_r = 1, L_B = 0.8, L_A = 0.32, L_R = 4, L_Z = 4 and L_H = 8. Impeller rotation velocity Ω is equal to 100 rpm. Reference time-scale and velocity are the rotation time, 1/Ω, and the blade tip velocity, $U_{tip} = \Omega L_r$. Fluid is water, with density $\rho = 10^3$ kg/m^3 and kinematic viscosity $\nu = 10^{-6}$ m^2/s. The Reynolds number, based on blade radius and blade tip velocity, $Re = \Omega L_r^2/\nu$, is 1636.
Boundary conditions are (i) no-slip at impeller blades and at external walls (enforced using the immersed boundary method) and (ii) free-slip at the top surface to mimic the presence of a flat free surface between water and upper air.
The flow field calculation has been extended from the previous simulation (Sbrizzai et al., 2006), up to 15 impeller revolutions, using a domain discretization of 97x102x192 grid points in the azimuthal, radial and axial direction respectively. A second simulation with a double number of grid nodes in each direction (about 16 millions points) has

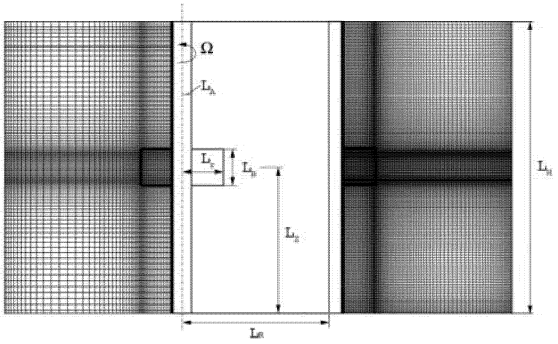

Figure 1 *Center*- Vessel geometry: dimensions are made dimentionless using the impeller radius Lr= 1.25 cm; *Left*- Computational grid used for flow field simulation (97x102x192) grid points in the azimuthal, radial and axial direction respectively; *Right*- Computational grid (193x203x383 grid nodes).

been performed to assess the accuracy of the method previously used and to test grid independence of turbulent related quantities.
As in Sbrizzai et al. (2006) we estimated the Kolmogorov length and time scales assuming that the relevant scales at which energy is introduced in the flow are the blade radius, L_r and the blade tip velocity, U_{tip} (Derksen, 2003). The Kolmogorov length scale have been calculated as $\eta=L_r /Re^{-3/4}$ = 48.5 μm and the Kolmogorov timescale as $\tau = 1/\Omega\ Re^{-0.5}$ = 2.35 10^{-3} s. These values have been used to assess the choice of space and time resolution by comparison with the minimum values of grid spacing.
In both configurations the mesh (see the left and right side of Figure 1) is non-uniform in the radial and axial directions, and is refined selectively in the regions where higher velocity gradients are expected. For both simulations, the time step used for flow field calculation is Δt = 1.25 10^{-4}s, i.e. About 1/18 of the Kolmogorov time scale. We started our calculation from a developed turbulent flow i.e. the last flow field obtained in our previous work.

2.1 Lagrangian tracking
We simulate the dispersion of three swarms made of O(10^4) solid particles of diameter 30 μm, 50 μm and 100μm and fluid-to-particle density ratio equal to ρ/ρp = 0.2. We calculate the trajectory of each particle by integrating explicitly over time the equation of motion using a time-step equal to one half of the characteristic time of the smallest particle. The assumptions for particle modeling are: (i) all particles are pointwise, non-interacting, non-deformable solid spheres; (ii) particle density is large compared to fluid density; (iii) the effect of the particles on the flow is neglected (iv) the equation of motion reduces to a balance of Stokes drag, gravity forces and particle inertia.

3. Results

A characteristic stirred tank flow pattern is clearly visible in Figure 2 (a) where the instantaneous flow field in a vertical section of the reactor, taken mid-way between two impeller blades is considered for visualization. Vectors represent radial and axial

velocity components in the plane. The discharge jet, issued radially from the impeller blade tip, splits in correspondence to the external wall, into two axial streams, upward and downward respectively, which form two main circulations having the shape of an upper and a lower toroidal vortex, respectively.

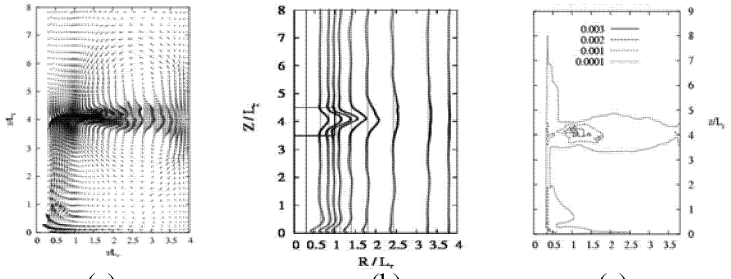

(a) (b) (c)

Figure 2: (a) Instantaneous flow field of radial and axial velocity components on a vertical plane taken mid-way between two impeller blades at the end of the simulation; (b) Time-averaged profiles of radial velocity component; (c) Iso-contours of angle-resolved averages of turbulent energy dissipation rate. Values are made dimensionless using reference time and velocity scales ($\varepsilon^{*}=\varepsilon/\Omega^{3}L_r^{2}$).

The difference in boundary conditions imposed at the bottom (no-slip wall) and at the top (free-slip wall) of the vessel is clearly visible in Figure 2 (b) where time averaged profiles of radial velocity are shown. High mean radial velocities are found at the impeller region and at the bottom of the tank where the fluid rubs against the no-slip surface generating negative mean velocity profiles.

Comparing the instantaneous flow field and Kolmogorov related quantities obtained with the coarse grid with those of the refined one (Figures not shown here) almost identical behavior has been achieved, confirming that the former is sufficient to obtain accurate prediction of the turbulent flow field in the vessel.

In our previous work (see Sbrizzai et al., 2006), we considered two swarms of 2 10^4 particles for each diameter (30 μm, 50 μm and 10μm), randomly distributed above and below the impeller plane ($z = L_H=4$) at starting time. Here, Lagrangian tracking has been performed starting our calculation from the particle position and velocity obtained at the end of the 3rd impeller revolution.

Figure 3 shows the evolution over time of the number of suspended particles. A particle is suspended when its distance from the bottom wall is greater than twice the particle diameter.

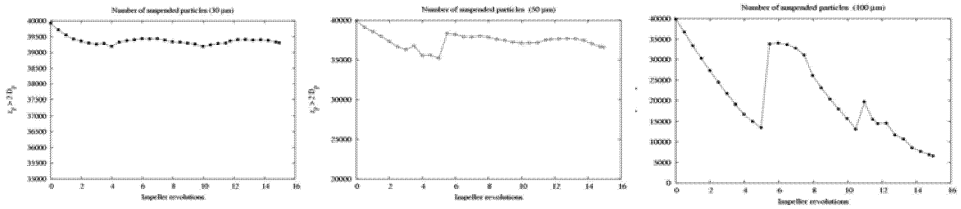

(a) (b) (c)

Figure 3: Number of suspended particles developing in time (a) 30μm; (b) 50μm and (c) 100μm.

For 30 µm particles (a) the number of suspended particles is constant over time, with particles homogeneously dispersed in the tank by a turbulence-driven diffusion process. For 50 µm (b) and 100 µm (c) particles, the number of suspended particles is decreasing over time, with almost periodic discontinuities which identify resuspension mechanisms. The observed behavior may be explained considering two main mechanisms: (i) gravitational settling, which promotes particle deposition at the vessel bottom and (ii) entrainment by a large-scale, intermittent, helical vortex generated by the Ekman pumping effect, which drives particles near the shaft from the bottom of the tank to the impeller blades.
Two resuspension peaks are, indeed, visible for 100µm particles in correspondence to the 5.8th impeller revolution and the 11.6th. For the first occurrence of this resuspension, we looked at the flow field structures which can be identified in the region between the impeller and the bottom wall.
Figure 4 (a) shows the precessional vortex present in this region using instantaneous vorticity isocontours to identify the helical structure around the shaft. Only a small cylinder below the impeller blades has been considered for visualization.

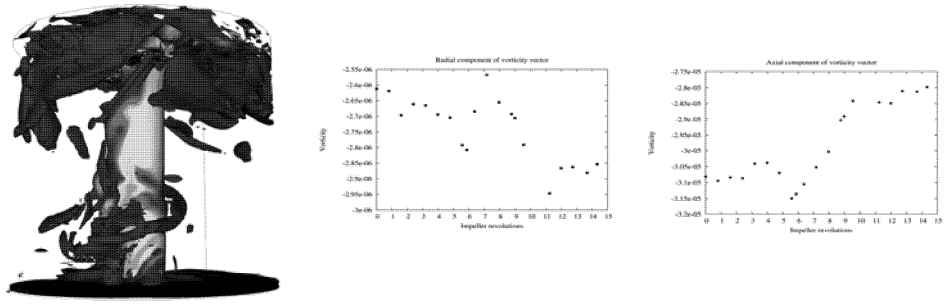

(a) (b) (c)

Figure 4: (a) Vorticity isocontours. A small cylinder below the impeller blades is considered for visualization; (b) Radial component of integral vorticity varying with time; (c) Axial component of intergal vorticity varying with time.

The helical vortex is generated when a radially converging fluid is produced in the boundary layer between a rotating flow and a solid boundary (Ekman layer). This kind of layer is present at the bottom of the tank close to the shaft, where, as visible in Figure 2 (c), high values of energy dissipation rate ε (calculated as $\varepsilon=2\nu S_{ij}S_{ji}$ where S_{ij} is the symmetric part of the velocity gradient tensor) are found and the fluid, brought in a counter clock-wise circulation by the impeller rotating motion, rubs against the flat no-slip bottom of the vessel.
From the results of our numerical simulation, we observed that the Ekman pumping is characterized by a specific frequency (f = 0.058 N, where N is the impeller speed). This is shown in Figure 4 (b) and (c) where the variation over time of volume integrated vorticity components are plotted. The same volume shown in Figure 4 (a) has been considered for integration. When the pumping effect becomes effective in re-suspending particles the radial and axial vorticity components show a negative peak.
The strict correlation between Ekman pumping event in the low portion of the tank and resuspension of particles indicates that the Ekman pumping plays a very important role in dispersing and re-suspending particles in such turbulent flows.

4. Conclusions

In this work, we used Direct Numerical Simulation and a Lagrangian tracking to simulate the behavior of three swarms of 40 000 solid particles (30 μm, 50 μm and 100 μm) to identify the role of large-scale flow structures in particle dispersion/resuspension dynamics in a stirred tank reactor. Mixing of particles is controlled by: (i) gravitational settling and (ii) Ekman pumping effect which is responsible for particle re-suspension toward the impeller blades.

Correlation between the pumping effect and vorticity of the flow proves the role of Ekman pumping in the re-suspension mechanisms.

5. References

Ducci, A., Yianneskis, M., 2007, Vortex tracking and Mixing Enhancement in Stirred Processes, AiChe Journal, 53, 305-315.

Galletti, C., Paglianti, A., Yianneskis, M., 2005, Observations on the significance of instabilities turbulence and intermittent motions on fluid mixing processes in stirred reactors, Chem. Eng. Sci., 60, 2317-2331.

Hartmann, H., Derksen, J.J., van den Akker, H.E.A., 2004, Macroinstability uncovered in a Rushton turbine stirred tank by means of LES, AiChE Journal, 50, 2383-2393.

Nikiforaki, L., Yu, J., Baldi, S, Genenger, B., Lee, K.C., Durst, F., Yianneskis, M., 2004, On the variation of precessional flow instabilities with operational parameters in stirred vessels, Chem. Eng. Journal, 102, 217-231.

Roussinova, V., Kresta, S.M., Weetman, R., 2003, Low frequency macroinstabilities in a stirred tank: scale-up and prediction based on large eddy simulations, Chem. Eng. Sci., 58, 2297-2311.

Sbrizzai, F., Lavezzo, V., Verzicco, R., Campolo, M., Soldati, A., 2006, Direct numerical simulation of turbulent particle dispersion in an unbaffled stirred-tank reactor, Chem. Eng. Sci., 61, 2843-2851.